

Improving of Thixotropic Properties of Bentonite Dispersions in Rheological Applications

Onur Eser KÖK^{1,a}, Hüseyin VAPUR^{2,b}, Yasin ERDOĞAN^{3,c}

¹İskenderun Technical University, Department of Petroleum and Natural Gas Engineering, Hatay, Türkiye

²Cukurova University, Department of Mining Engineering, Adana, Türkiye

³Republic of Turkey, Ministry of Energy and Natural Resources, Ankara, Türkiye

^aORCID: 0000-0002-7061-2921; ^bORCID: 0000-0003-4438-3982; ^cORCID: 0000-0002-2314-5216

Article Info

Received : 03.09.2024

Accepted : 25.03.2025

DOI: 10.21605/cukurovaumfd.1665824

Corresponding Author

Onur Eser KÖK

oeser.kok@iste.edu.tr

Keywords

Bentonite

Activation

Shear stress

Viscosity

Rheological modelling

How to cite: KÖK, O.E., VAPUR, H., ERDOĞAN, Y., (2025). Improving of Thixotropic Properties of Bentonite Dispersions in Rheological Applications. Cukurova University, Journal of the Faculty of Engineering, 40(1), 49-60.

ABSTRACT

In this study, the improvement of the rheological properties of bentonites by alkaline activation was investigated. The characterizations of the samples used in the study were determined by X-ray fluorescence spectroscopy (XRF), particle size distribution (PSD), cation exchange capacity (CEC), specific surface area (SSA) analysis and scanning electron microscopy (SEM) images. The rheological properties of the suspensions were determined by apparent viscosity (AV), plastic viscosity (PV), yield point (YP) and gel strength (GS) measurements. In addition, static filtration analysis was performed and thixotropic properties were determined by shear thinning index (STI) and thixotropy index (TI) calculations. Rheological flow parameters were calculated using the least squares method (LSM) and the model equations were created according to the Herschel-Bulkley flow model (HBM). As a result of the analyzes, it was determined that the alkaline activation process improved the rheological and thixotropic properties of bentonite dispersions. Also, the rheogram curves indicate that the suspensions showed a shear-thinning flow behavior. In the HBM evaluation, it was determined that the best flow properties belonged to EB (0.9987 R²) in raw samples and NB (0.9985 R²) in activated samples.

Reolojik Uygulamalarda Bentonit Dispersiyonlarının Tiksotropik Özelliklerinin İyileştirilmesi

Makale Bilgileri

Geliş : 03.09.2024

Kabul : 25.03.2025

DOI: 10.21605/cukurovaumfd.1665824

Sorumlu Yazar

Onur Eser KÖK

oeser.kok@iste.edu.tr

Anahtar Kelimeler

Bentonit

Aktivasyon

Kayma gerilmesi

Viskozite

Reolojik modelleme

Atf şekli: KÖK, O.E., VAPUR, H., ERDOĞAN, Y., (2025). Reolojik Uygulamalarda Bentonit Dispersiyonlarının Tiksotropik Özelliklerinin İyileştirilmesi. Çukurova Üniversitesi, Mühendislik Fakültesi Dergisi, 40(1), 49-60.

ÖZ

Bu çalışmada, bentonitlerin reolojik özelliklerinin alkali aktivasyonla iyileştirilmesi araştırılmıştır. Çalışma kapsamında kullanılan numunelerin karakterizasyonları X-ışını floresans spektroskopisi (XRF), tanecik boyut dağılımı (PSD), kation değişim kapasitesi (CEC), spesifik yüzey alanı (SSA) analizleri ve taramalı elektron mikroskobu (SEM) görüntüleri ile belirlenmiştir. Süspansiyonların reolojik özellikleri görünür viskozite (AV), plastik viskozite (PV), kopma noktası (YP) ve jel kuvveti (GS) ölçümleri ile belirlenmiştir. Ayrıca statik filtrasyon analizi yapılmış olup, tiksotropik özellikleri kayma incelme indeksi (STI) ve tiksotropi indeksi (TI) hesaplamaları ile belirlenmiştir. Reolojik akış parametreleri en küçük kareler yöntemi (EKK) kullanılarak hesaplanmış olup, model denklemleri Herschel-Bulkley akış modeline (HBM) göre oluşturulmuştur. Yapılan analizler sonucunda alkali aktivasyon işleminin bentonit dispersiyonlarının reolojik ve tiksotropik özelliklerini iyileştirdiği belirlenmiştir. Ayrıca, reogram eğrileri süspansiyonların kayma incelme davranışı gösteren bir akış gösterdiğini ifade etmektedir. HBM reolojik model değerlendirmesinde en iyi akış özelliklerinin ham numunelerde EB kodlu numuneye (0,9987 R²), aktivasyonlu numunelerde ise NB kodlu numuneye (0,9985 R²) ait olduğu belirlenmiştir.

1. INTRODUCTION

Bentonites that member of smectite type clay minerals come front among the others due to can shows gel-form at low concentrations [1-4]. They vary differ types according to dominant ions in contain as sodium, calcium and mix types. Each of them shows differ gel function and swelling mechanism. Thus, they do not always show the same properties [5-7]. Each type bentonites are preferred according to differ usage areas considering the general properties. Sodium type ones are widely used because of they can occure more viscous suspensions than others. For this reason, the conversion studies of calcium and mix types to sodium type continues from past to present. Considering the suspension properties, bentonites are more preferred and used especially in drilling operations than others [8-11].

Bentonites used as a major additive material in drilling operations due to swelling and thixotropy (TP) properties [12]. Although there are many drilling fluid systems, water-based is the most widely used [13]. It has a significant cost effect (~15-20%) on the drilling cost and has important duties for well such as removing the cuttings from bottom to surface, cooling bit, provide stability, controlling formation pressure, preventing corrosion and suspending cuttings [14,15]. In drilling, drilling fluid must have some flow properties to perform tasks because of differences in well and surface (pressure, temperature, rock properties of drilled). With these properties, rheology of drilling fluid is controlled. To controlling rheology of drilling fluid, some materials (chemicals, organics, and polymers) is added into system [16]. However, these materials increase the drilling cost. Therefore, the bentonite added drilling fluids comes to the fore in controlling the flow properties of drilling mud because it is cheap and has abundant reserves. However, the specifications of bentonite used are also important in controlling drilling fluid rheology. Bentonites, has high swelling capacity and low filtrate volume, should be preferred. Thus, more viscous drilling fluid can be obtained. Therefore, either bentonite with good properties should be used or the rheological properties of bentonite should be improved [17].

In this study, the rheological and thixotropic properties of raw and activated bentonites were investigated. Flow properties of the muds like apparent viscosity (AV), plastic viscosity (PV), yield point (YP), gel strength (GS) (10 sec. and 10 min) and filtration were evaluated. Then, usability of bentonites was determined as drilling fluid additive. Also, shear stress (SS) values of the muds at different shear rates (SR) were measured with rotational viscometer and investigated according to Herschel-Bulkley (HB) rheological model according to least squared method (LSM) with MatLab.

2. MATERIAL AND METHOD

The bentonite samples that were used the experiments were collected different region and companies. WB was taken from HALLIBURTON, EB and RB were taken from CANBENSAN, NB was taken from RBS and UB was taken from BENTAS.

The activation process was applied using with sodium carbonate (Na_2CO_3) and magnesium oxide (MgO) according to dry alkaline method [18]. This activation method was applied to the concentrated bentonites, which are obtained from grinding the WB, EB, RB, NB and UB and sieved under 150 μm particle size. Then, drying process was applied under at 105 $^\circ\text{C}$ and 120 min. conditions so that remove the free water molecules. After this process, bentonite samples were cooled and were taken into mixing machine and deionized water sprayed (min. 15 minutes) until humidity reached at 40% when mixing continued. Then, Na_2CO_3 was added the ratio of wt.2.5% to the samples, which been the form like dense paste, and mixing was applied for 15-20 minutes so that homogenization. They were turned into round pieces with a diameter of 4-5 cm for the drying and holding process to be efficient and kept for 8-9 weeks for the exchange of Na^+ cations. Afterwards, the grinding was made using with planetary ball mill. As a result of the grinding, the micronize particle sized samples were sieved to be lower than 75 μm . After the sieving MgO was added as ratio of 0.5 wt% with dry mixing. The activation was completed as a result of these steps.

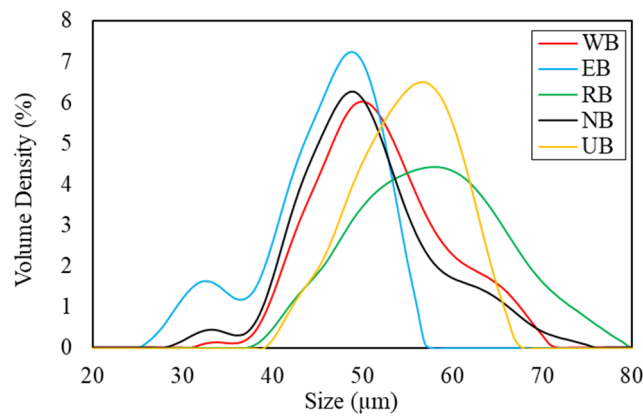
The chemical compositions of the bentonite samples were detected X-ray fluorescence (XRF) analysis with MINIPAL 4 and results obtained from Kk et al. [19] (see Table 1). The particle size distribution (PSD) of samples were analysed by Malvern Panalytical Mastersizer 3000 and results given in Figure 1. Here, the samples were grinding with a laboratory scale ball mill. The particle size distribution of bentonites (see Table 2) were provided to be compatible with API 13A standard ($d_{90} < 75 \mu\text{m}$) [20].

Table 1. Chemical analysis of bentonites

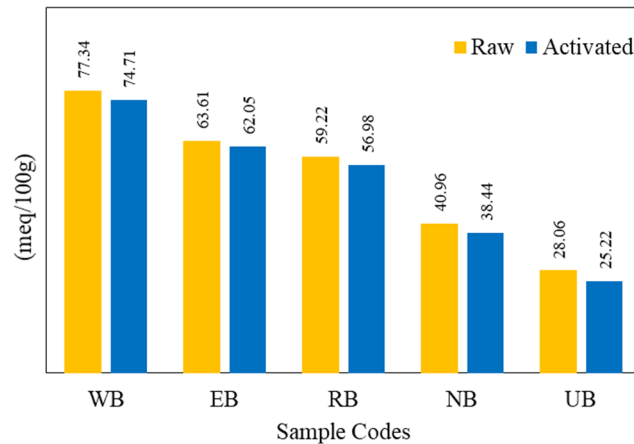
Raw Samples	SiO ₂	Al ₂ O ₃	Fe ₂ O ₃	CaO	K ₂ O	MgO	Na ₂ O	TiO ₂	MR
WB	64.27	15.51	5.62	1.12	0.52	0.03	2.79	0.24	2.88
EB	56.71	16.27	7.12	5.35	1.42	0.17	1.59	0.67	0.55
RB	52.13	14.34	11.20	5.11	1.76	0.23	2.82	1.69	0.86
NB	52.84	14.44	9.70	6.43	1.20	0.16	1.93	1.42	0.48
UB	65.69	16.37	1.09	4.91	0.49	0.04	0.91	0.18	0.28
Activated Samples	SiO ₂	Al ₂ O ₃	Fe ₂ O ₃	CaO	K ₂ O	MgO	Na ₂ O	TiO ₂	MR
WB	65.98	16.31	5.57	1.1	0.61	0.11	2.99	0.34	2.97
EB	58.84	15.67	7.53	4.33	2.01	0.21	2.85	0.81	1.07
RB	52.71	15.40	10.98	4.04	1.97	0.37	3.17	1.69	1.17
NB	56.44	13.51	9.67	3.91	1.55	0.21	3.69	1.12	1.27
UB	63.79	14.53	1.77	4.00	1.19	0.11	2.99	0.56	1.02

Table 2. PSD of the raw bentonites

Sample	d ₁₀	d ₅₀ (μ m)	d ₉₀
WB	2.36	6.49	26.5
EB	0.81	3.65	7.91
RB	3.66	14.4	60.0
NB	1.99	5.34	24.2
UB	3.73	10.7	25.8

**Figure 1.** Particle size distribution of bentonite samples

The cation exchange capacity (CEC) of the samples were calculated using methylene blue solution according to API 13I standard [21] and given in Figure 2.

**Figure 2.** CEC values of the bentonites

The specific surface area (SSA) of the samples were determined with Brunauer-Emmett-Teller (BET) analysis using N₂ adsorption-desorption measurements by Costech Sorptometer 1042 and results given in Figure 3.

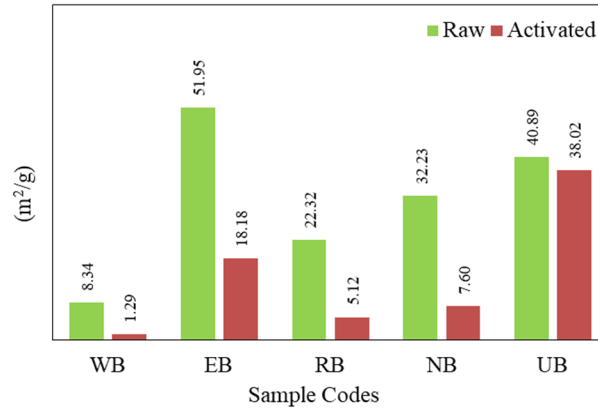


Figure 3. SSA values of bentonites

The scanning electron microscope (SEM) images of the samples were obtained with using Quanta FEG 650 scanning electron microscope for morphological evaluations. The images of raw and activated bentonites were shown in Figure 4 and Figure 5, respectively.

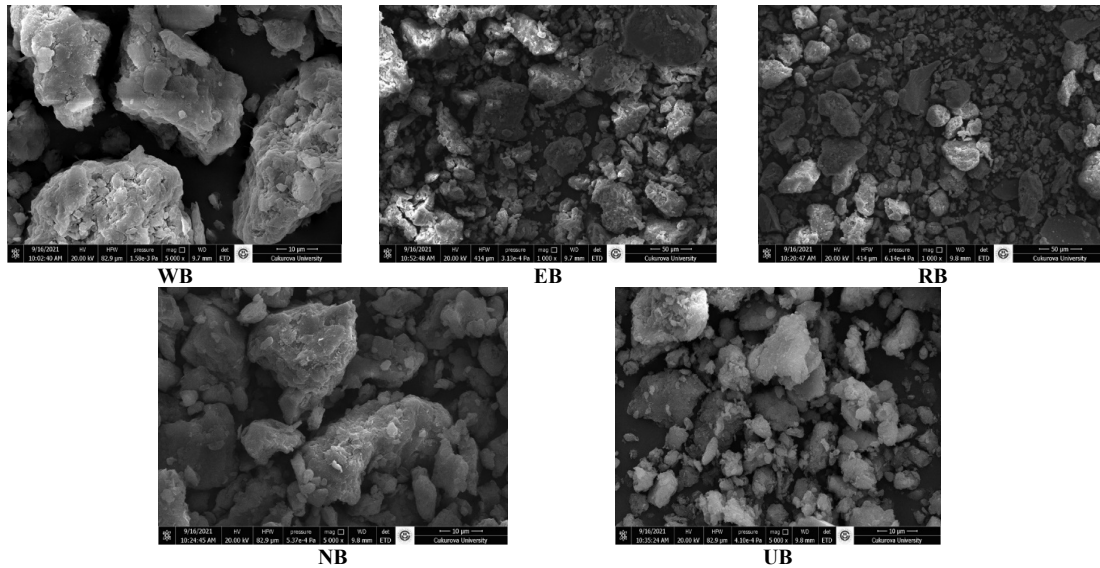


Figure 4. SEM images of the raw bentonites

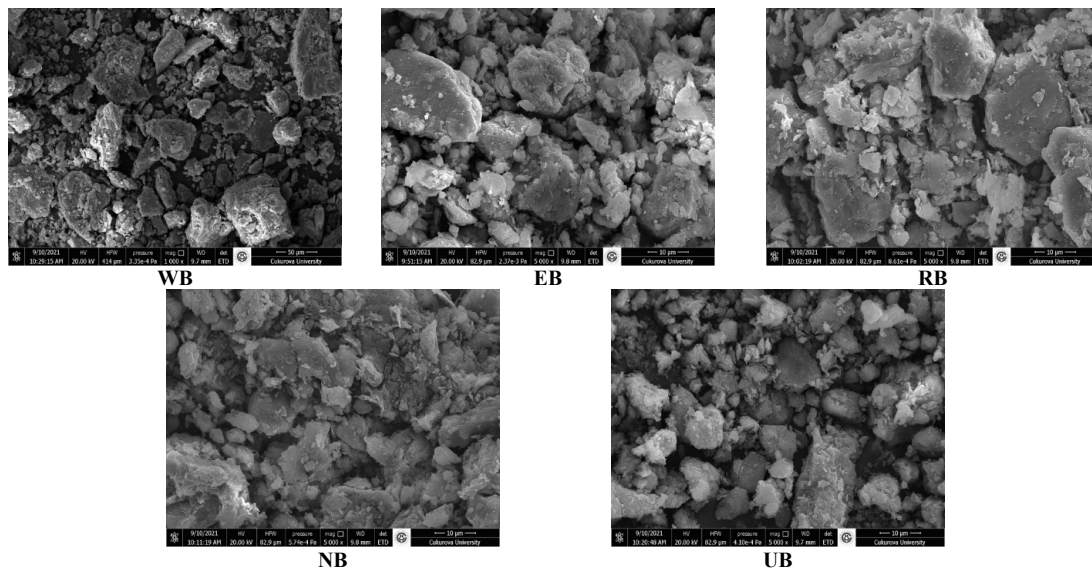


Figure 5. SEM images of the activated bentonites

The drilling mud samples were prepared using wt. 6% suspension ratio according to API 13A standard. In addition, the pH of all samples was be ensured range between 7.7-8.5.

Rheological properties of the muds were determined with a rotational viscometer (OFITE Model 800) by considering SS, PV, YP and AV. The viscometer equipped with six speeds as 600, 300, 200, 100, 60, 30, 6 and 3 (rpm). After reading and recording the values, Equations 6-7 were applied.

The PV and YP are determined in a concentric cylinder rotary viscometer as high accuracy. The essential elements of viscometers are rotor and bob, and in this study, R1-B1 rotor-bob system was used. As a work system, an outer cup rotates concentrically around an inner cylinder or bob, that is suspended from a torsion wire. A dial affixed and a pointer are used to measure the angle at which the wire rotates. When the cup is rotated, the bob rotates together with up to the torque in the wire creates a SS at the bob surface higher than the shear strength of the plastic structure [22]. And definition equation is given below.

$$\frac{T_0}{2\pi R_b^2 h} = \tau_0 \quad (1)$$

T_0 : torque at the yield point; R_b : bob radius; h : bob's effective height

The yield point (τ_0) is defined with the intercept. Also, T_2 , is the extrapolation of the curve linear portion on the torque axis. It is given with above equation in condition that $\omega=0$. Then;

$$\frac{T_2}{4\pi h} \left(\frac{1}{R_b^2} + \frac{1}{R_c^2} \right) = \tau_0 \ln \frac{R_c}{R_b} \quad (2)$$

There are a many commercially available and suitable viscometer. Some of them can be used for drilling muds and they are similar in work principle. All are based on a design by Savins and Roper [23], which enables the plastic viscosity (PV) and yield point (YP) to be calculated from 600 and 300 rpm. The underlying theory is as follows:

$$\mu_p = \frac{A\theta - B\tau_0}{\omega} \quad (3)$$

where A: spring constant; B: conversion factor; ω : rotor speed (rpm)

Then,

$$\mu_p = PV = A \left(\frac{\theta_1 - \theta_2}{\omega_1 - \omega_2} \right) \quad (4)$$

θ_1 : dial reading at ω_1 rpm; θ_2 : dial reading at ω_2 rpm; PV: plastic viscosity

$$\tau_0 = YP = \frac{A}{B} \left[\theta_1 - \left(\frac{\omega_1}{\omega_1 - \omega_2} \right) (\theta_1 - \theta_2) \right] \quad (5)$$

θ_1 : dial reading at ω_1 rpm; θ_2 : dial reading at ω_2 rpm; PV: plastic viscosity; YP: yield point.

Then,

Equations 4 and 5 then simplify to;

$$PV = \theta_1 - \theta_2 \quad (6)$$

$$YP = \theta_2 - PV \quad (7)$$

To provide these parameters, R_b and R_c were chosen so that, with an annulus width of about 1mm, the value of $A=B$ would be 300, ω_2 was therefore 300 rpm, and ω_1 , 600 rpm. Then, the specifications enabled Equation 6 to give the PV (cP), and Equation 7 to give the YP (lb/100ft²). In addition, Equation 8 to give the apparent viscosity (AV) in centipoise (cP).

$$AV = \frac{300 \times \theta_{600}}{600} = \frac{\theta_{600}}{2} \quad (8)$$

GS of the muds were measured by reading maximum dial reading at 3 rpm for at 10 sec. and 10 min. with rotational viscometer. Before each measurement, the muds were stirred for dispersion (min. 10 sec. at 600 rpm).

Filtration properties of the muds were determined with fluid loss test by using API filter press test kit under 100 ± 5 PSI nitrogen pressure for 30 min. at room temperature.

TP properties of the muds were determined according to the shear thinning index (STI) and thixotropy index (TI) given in Equations 9-10.

$$STI = \frac{\theta_3}{\theta_{300}} \quad (9)$$

$$TI = \frac{\theta_{600min}}{\theta_{600max}} \quad (10)$$

Rheograms of the muds were determined according to SS values at different SR. Also, the rheological parameter estimations were performed according to HB model given in Eq. 11. Model parameters were determined using least squares method of Matlab™ and the coefficient of determination (R) indicator.

$$\tau = \tau_y + k\gamma^n \quad (11)$$

Where, τ and γ are the SS and SR, respectively. Others are rheological parameters of the model.

3. RESULTS AND DISCUSSION

3.1. Characterization Results

Mass ratio (MR) values were calculated using the XRF results by $\text{Na}_2\text{O} + \text{K}_2\text{O} / \text{CaO} + \text{MgO}$ equation (Na-Ben: $\text{MR} > 1$, Na/Ca-Ben: $0.35 < \text{MR} < 1$, Ca-Ben: $\text{MR} < 0.35$). Results showed that WB is Na-Ben, EB, RB and NB are Na/Ca-Ben and UB is Ca-Ben in raw samples. However, all samples were determined as Na-Ben after the activation.

The PSD results showed that all sampled were provided to API standarts ($d_{90} < 75 \mu\text{m}$). Also, the highest and lowest values were measured as $60.0 \mu\text{m}$ and $7.91 \mu\text{m}$ from RB and UB, respectively. Other raw bentonite samples values varied between $24\text{-}27 \mu\text{m}$.

In the CEC analyzes, its seen that activated samples has lower exchangeable cations than raw ones (see Fig. 3). Because of the hydration ability, Na^+ cations easily replaced the Ca^{2+} cations. Considering the cation exchange tendencies ($\text{Mg}^{2+} > \text{Ca}^{2+} > \text{K}^+ > \text{Na}^+$), there were a decrease in the CEC values of all samples due to Na^+ were lower than Ca^{+2} [24,25]. However, due to the low concentration (2.5% by weight) of soda activation, a significant change was not determined.

SSA values of the raw bentonite samples were determined lower than raw samples (see Fig. 4). With the Na^+ entered between the particles and settled in the spaces between the layers, micro cracks filled. Thus, porosity and permeability decreased [26].

According to the SEM images of the raw bentonites, it is seen that the samples have thin and porous form. These images are expressed as tulle morphology and associated with smectite group clays. Also, it is seen that the samples have irregular dimension and shape of all. Additionally, it is clearly seen that some particles come together to form larger pieces in the form of lumps. Moreover, it is seen that the SEM images of activated bentonites are in similar form to the raw ones. In addition, it is determined that the dispersion tendencies of the lumps increased for all of the samples after the activation process and moderate dispersions occurred.

3.2. Analyzing of the Viscosity, GS and Filtration Results

AV, PV and YP analyzes were applied for determining to flow properties of the muds. AV was measured for real time viscosity estimation and flowability determination; PV was measured for solid content effect on viscosity; and YP was measured for transition initial SS from static to dynamic phase. Analyzes results given in Figure 6 and Figure 7.

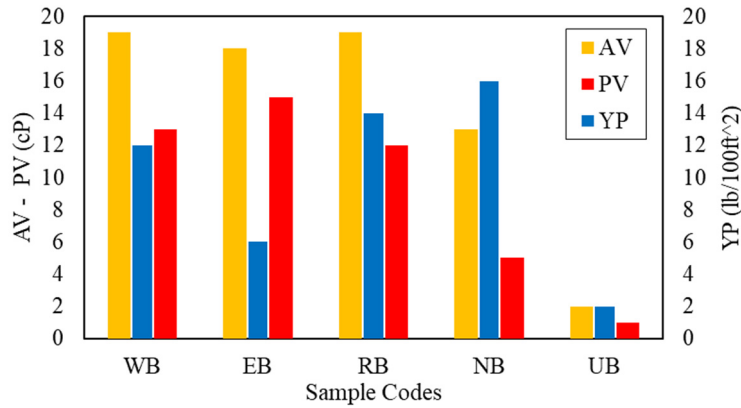


Figure 6. Viscosity results of raw bentonites

The maximum AV values with 19 cP were recorded from WB and RB in raw samples. Also, the minimum value was obtained with 2 cP from UB. When evaluated the activated samples, AV values were recorded 25 cP from NB as highest and 9 cP from UB as lowest. Evaluating the activation effect, it was seen that AV increased with activation for WB, EB and RB as 23.5%, 22.2% and 31.5% respectively. Also, it was noticed that NB reached nearly twice the value and UB reached nearly four times. According to the API 13A standard, it should have an AV of at least 15 cP to be used as drilling mud. For raw samples, it was determined that WB, EB and RB suitable for API with as 19 cP, 18 cP and 19 cP, respectively. For activated samples, it is determined that all muds suitable for the standard except UB (9 cP).

The highest PV was recorded from EB with 15 cP and lowest with 1 cP from UB. In the activated samples, PV were recorded 16 cP from WB and NB as highest and 3 cP from UB as lowest. When evaluated the activation effect, an increase observed for WB, NB and UB by 1.23, 3.2 and 3 times respectively. A decrease observed for EB and RB by 33.3% and 8.3%.

YP obtained as maximum and minimum from NB and UB with 16 lb/100ft² and 2 lb/100ft², respectively in raw suspensions. In addition, the highest values in activated samples were from EB and RB with 24 lb/100ft²; the lowest was determined as 10 lb/100ft² from WB. After the activation, an increase in YP observed all samples except WB (decrease 16.6%). It is determined that these increases were highly in some samples such as 18 lb/100ft² for EB, 10 lb/100ft² for RB, 9 lb/100ft² for UB. Also 2 lb/100ft² increase observed in NB.

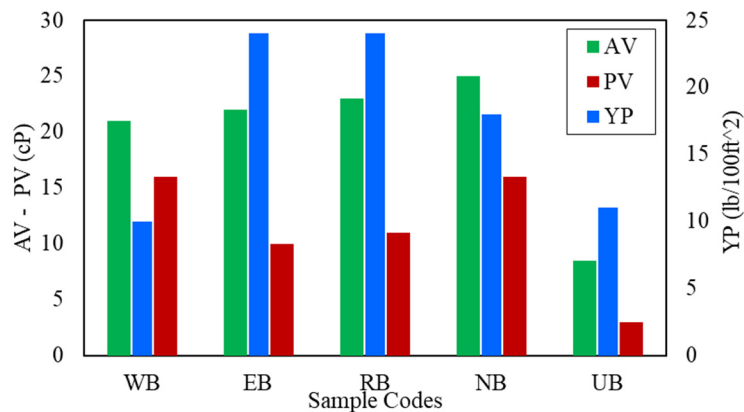


Figure 7. Viscosity results of activated bentonites

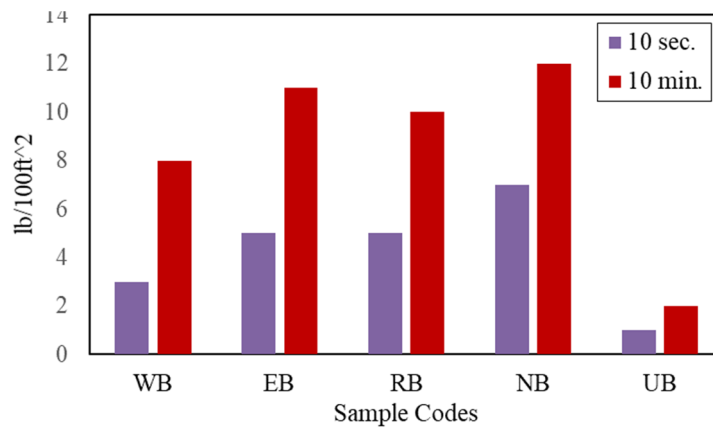


Figure 8. GS of raw bentonites

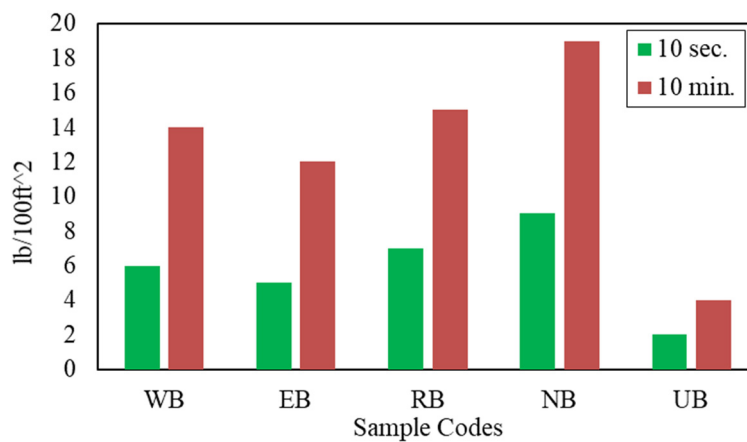


Figure 9. GS of activated bentonites

GS analyzes were applied for determined to TP properties of the muds in non-flow times and results given in Figure 8 and Figure 9. GS results (10 sec.) of the muds prepared with raw bentonites showed that ranges from 1 lb/100ft² (UB) to 7 lb/100ft² (NB). Also, increases were determined after the activation and these increases ranges from 1 lb/100ft² to 3 lb/100ft² except EB. There was no determined any changes in EB with activation (5 lb/100ft²). In addition, GS results (10 min.) of the muds (prepared with raw bentonites) showed that ranges from 2 lb/100ft² (UB) to 12 lb/100ft² (NB). In addition, increases were determined ranges from 1 lb/100ft² to 7 lb/100ft² after the activation. Results showed that alkaline activation increased the GS. With the cation exchange, swelling properties of the bentonites improved and more water molecules settled into the layers.

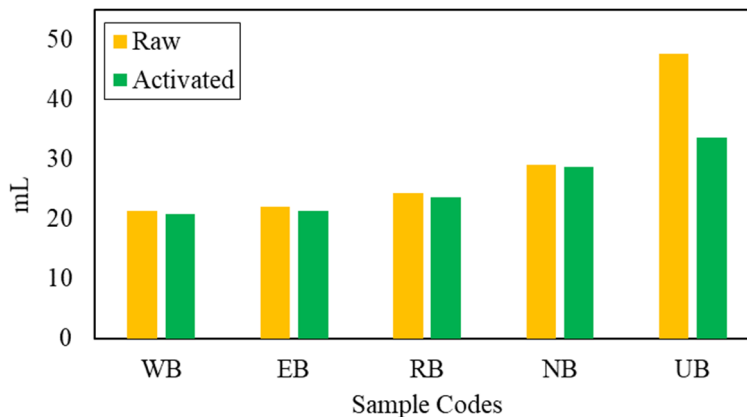


Figure 10. Filtrate volumes of bentonites

In the filtration analysis, the lowest filtrate volume was determined from WB (21.4 mL) and highest from UB (47.6 mL) in the muds prepared with raw bentonites. In addition, 20.9 mL (WB) and 33.7 mL (UB) filtrates were determined as maximum and minimum after the activation (see Fig. 10). Results showed that filtrates decreased with the activation. With the increase in swelling capability, a thickening occurred in the mud cake and the filtrate in the mud was less able to pass into the cylinder. These decreases were measured as 2.33% for WB, 3.62% for EB, 3.28% for RB, 1.03% for NB and 29.2% for UB.

3.3. Analyzing of the TP

TP analyzes of the suspensions were evaluated in two sections as STI and TI. These analyzes were associated with thixotropy of the suspensions. Increasing of STI and decreasing of TI indicate improved TP. STI and TI values are given in Figure 11 and Figure 12, respectively.

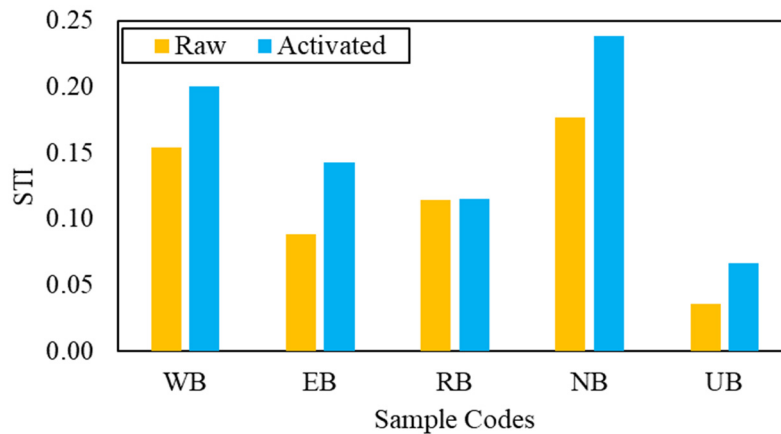


Figure 11. STI values of bentonites

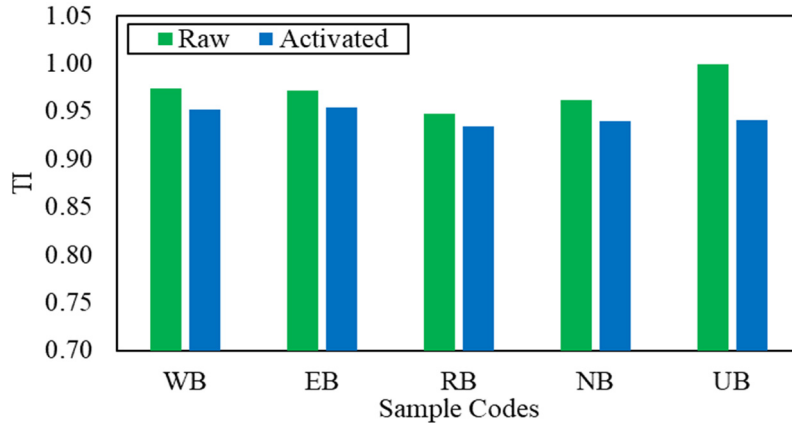


Figure 12. TI values of bentonites

In the STI analysis, it was observed that there was an increasing for all suspensions after the activation. STI increased 33.3%, 55.5%, 9.1%, 33.3% and 75% for WB, EB, RB, NB and UB respectively. Also, in the TI analysis, it was observed that there was a decreasing. These decreasing ratios were 2.06%, 2.06%, 2.1%, 2.08% and 6% for WB, EB, RB, NB and UB respectively. These results showed that TP improved, and activation get positive effect.

3.4. Rheology and Model Determination

The rheograms (also named as flow curves) were prepared with SS values versus the SR (Figure 13 and Figure 14). Rheology profiles were determined according to these flow curves. According to the results, it was clearly seen that the muds show yield pseudoplastic flow. Also, rheograms showed that the SS values measured at low SR (<200 rpm) are close to each other, the difference is greater at high SR (>300 rpm). In addition, SS values increased at all SR after the activation.

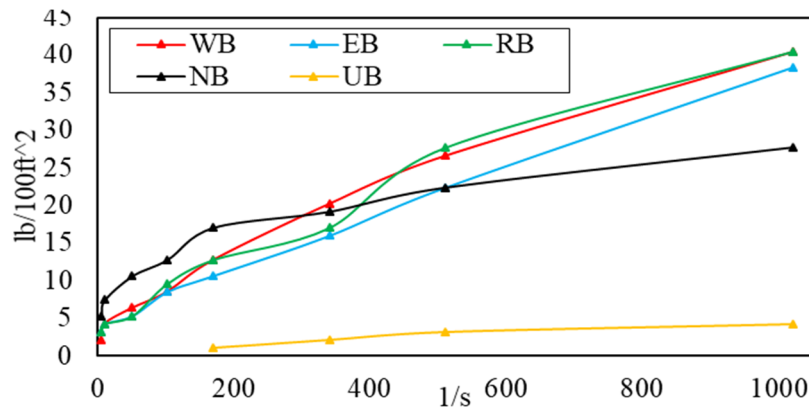


Figure 13. Rheograms of raw bentonites

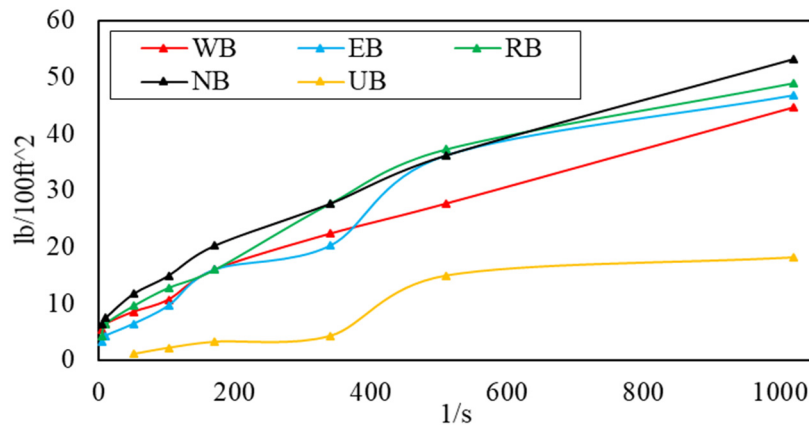


Figure 14. Rheograms of activated bentonites

Model parameters of the muds calculated using LSM and results given Table 3 and Table 4. According to the results, it was determined that the EB showed the best suitable result with 0.9987 R^2 for HBM among the raw bentonite suspensions. Also, the UB showed the most unsuitable result with 0.9160 R^2 . Among the activated bentonite suspensions, it was determined that the NB showed the best suitable result with 0.9985 R^2 value for HBM. Also, the UB showed the most unsuitable result with 0.7958 R^2 .

Table 3. Model parameters of raw samples

Samples	Model parameters	Model equation	Statistical results
WB	$k = 0.511$ $n = 0.628$ $\tau_y = 0.548$	$\tau = 0.548 + 0.511 \cdot \gamma^{0.628}$	$R^2 = 0.9959$ RMSE = 0.7840
EB	$k = 0.082$ $n = 0.875$ $\tau_y = 3.205$	$\tau = 3.205 + 0.082 \cdot \gamma^{0.875}$	$R^2 = 0.9987$ RMSE = 0.4079
RB	$k = 0.761$ $n = 0.570$ $\tau_y = 0.458$	$\tau = 0.458 + 0.761 \cdot \gamma^{0.570}$	$R^2 = 0.9773$ RMSE = 1.8424
NB	$k = 3.087$ $n = 0.314$ $\tau_y = 0.411$	$\tau = 0.411 + 3.087 \cdot \gamma^{0.314}$	$R^2 = 0.9931$ RMSE = 0.5967
UB	$k = 0.288$ $n = 0.415$ $\tau_y = 1.034$	$\tau = 1.034 + 0.288 \cdot \gamma^{0.415}$	$R^2 = 0.9160$ RMSE = 0.9436

Table 4. Model parameters of activated samples

Samples	Model Parameters	Model Equation	Statistical Results
WB	k = 0.144 n = 0.811 $\tau_y = 5.321$	$\tau = 5.321 + 0.144 \cdot \gamma^{0.811}$	R ² = 0.9971 RMSE = 0.6748
EB	k = 3.938 n = 0.372 $\tau_y = 8.239$	$\tau = 8.239 + 3.938 \cdot \gamma^{0.372}$	R ² = 0.9316 RMSE = 3.9095
RB	k = 3.402 n = 0.394 $\tau_y = 5.075$	$\tau = 5.075 + 3.402 \cdot \gamma^{0.394}$	R ² = 0.9651 RMSE = 2.8064
NB	k = 0.655 n = 0.622 $\tau_y = 4.136$	$\tau = 4.136 + 0.655 \cdot \gamma^{0.622}$	R ² = 0.9985 RMSE = 0.5777
UB	k = 3.350 n = 0.280 $\tau_y = 7.991$	$\tau = 7.991 + 3.350 \cdot \gamma^{0.280}$	R ² = 0.7958 RMSE = 2.9609

4. CONCLUSION

The aim of this study was to determine the rheological and filtration properties of bentonites and to improve flow properties for drilling applications by dry alkaline activation. For this purpose, comprehensive works were conducted in experiments. It was determined that the activation showed a positive effect on the rheological properties of bentonites such as AV, PV, YP, GS, STI and TI. The TP of the drilling fluids were improved, and fluid losses were decreased. Alkaline activation of bentonites with 2.5 wt.% Na₂CO₃ and 0.5 wt.% MgO improved the flow properties of the muds. Therefore, activated bentonites usability in oilfields can be increased and provided less use of other high costly rheology additives (such as PAC and polymers) that increase viscosity. Also, some raw bentonites can be used directly in drilling fluids, however it was determined that it better results were obtained with the activation. Flow properties of drilling fluids in wellsite can be determined with the development of computer solutions and analytical programs easily. Thus, dynamic flow profiles of the drilling fluids in the well can be estimated without practical applications with high accuracy. In the rheological model evaluation according to HBM, the results showed that the EB is the most suitable with 0.9987 R² value among the raw bentonite samples, the NB is the most suitable with 0.9985 R² value among the activated ones. Thus, it will be possible to prepare less costly and more convenient drilling muds with this samples.

5. ACKNOWLEDGEMENT

This study supported by Cukurova University Scientific Research Projects Department with the Project Code FDK-11786. Also, the scientific results that given in this study obtained from the scope of PhD thesis of first author within Cukurova University Institute of Natural and Applied Sciences.

6. REFERENCES

1. Koutsopoulo, E., Christidis, G.E. & Marantos, I. (2016). Mineralogy, geochemistry and physical properties of bentonites from the Western Thrace Region and the islands of Samos and Chios, East Aegean, Greece. *Clay Minerals*, 51, 563-88.
2. Luckham, P.F., Rossi, S. (1999). The colloidal and rheological properties of bentonite suspensions. *Advances in Colloid and Interface Science*, 82(1-3), 43-92.
3. Mpofu, P., Addai-Mensah, J. & Ralston, J. (2004). Flocculation and dewatering behaviour of smectite dispersions: effect of polymer structure type. *Minerals Engineering*, 17(3), 411-23.
4. Shakeel, A., Safar, Z., Ibanez, M., Van Paassen, L. & Chassagne, C. (2020). Flocculation of clay suspensions by anionic and cationic polyelectrolytes: a systematic analysis. *Minerals*, 10(11), 999-1023.

5. Bergaya, F., Lagaly, G. (2013). Handbook of clay science: Developments in clay science (2nd ed.). Elsevier, United Kingdom.
6. Zhou, C., Tong, D. & Yu, W. (2019). Smectite nanomaterials: preparation, properties, and functional applications, nanomaterials from clay minerals. Elsevier, United Kingdom.
7. Hwang, J., Pini, R. (2019). Supercritical CO₂ and CH₄ uptake by illite-smectite clay minerals. *Environmental Science & Technology*, 53(19), 11588-11596.
8. Abdou, M.I., Ahmed, H.S. (2011). Effect of particle size of bentonite on rheological behavior of the drilling mud. *Journal of Petroleum Science and Technology*, 29, 2220-2233.
9. Abdollahi, M., Pourmahdi, M. & Nasiri A.R. (2018). Synthesis and characterization of lignosulfonate/acrylamide graft copolymers and their application in environmentally friendly water-based drilling fluid. *Journal of Petroleum Science and Engineering*, 171, 484-494.
10. Xiang, G., Ye, W., Xu, Y. & Jalal, F. E. (2020). Swelling deformation of Na-bentonite in solutions containing different cations. *Engineering Geology*, 277, 105757.
11. Harjupatana, T., Miettinen, A. & Kataja, M. (2022). A method for measuring wetting and swelling of bentonite using X-ray imaging. *Applied Clay Science*, 221, 106485.
12. Afolabi, R.O., Orodu, O.D. & Efeovbokhan V.E. (2017). Properties and application of Nigerian bentonite clay deposits for drilling mud formulation: recent advances and future prospects. *Applied Clay Science*, 143, 39-49.
13. Lagaly, G. (2006). Handbook of clay science: developments in clay science (2nd ed.). Elsevier, United Kingdom.
14. Goel, P.N., Anand, A., Anand, S.R., Jha, K. & Richhariya, G. (2022). Development of cost-effective drilling fluid from banana peel pectin and fly ash for loss circulation control. *Materials Today: Proceedings*, 62, 4177-4181.
15. Erdoğan, Y., Kök O.E. (2019). Production and characterization of nanobentonite from sodium bentonite with mechanical grinding. *Fresenius Environmental Bulletin*, 28(11), 8141-8150.
16. Agwu, O.E., Akpabio, J.U., Ekpenyong, M.E., Inyang, U.G., Asuquo, D.E., Eyoh, I.J. & Adeoye O.S. (2021). A comprehensive review of laboratory, field and modelling studies on drilling mud rheology in high temperature high pressure (HTHP) conditions. *Journal of Natural Gas Science and Engineering*, 94, 104046.
17. Altun, G., Osgouei, A.E. (2014). Investigation and remediation of active-clay contaminated sepiolite drilling muds. *Applied Clay Science*, 102, 238-245.
18. Karagüzel, C., Çetinel, T., Boylu, F., Çinku, K. & Çelik, M.S. (2010). Activation of (Na, Ca)-bentonites with soda and MgO and their utilization as drilling mud. *Applied Clay Science*, 48, 398-404.
19. Kök, O.E., Vapur, H. & Erdoğan, Y. (2023). Rheological behavior of activated bentonite suspensions and estimation of flow models using least squares method. *Geoenergy Science and Engineering*, 230, 212181.
20. API SPEC 13-A, (2010). Specification for Drilling Fluids Materials. American Petroleum Institute, Washington.
21. API SPEC 13-I, (2020). Laboratory Testing of Drilling Fluids. American Petroleum Institute, Washington.
22. Caenn, R., Darley, H.C. & Gray, G.R. (2011). Composition and properties of drilling and completion fluids. Gulf professional publishing, Elsevier.
23. Savins, J.G., Roper, W.F. (1954). A direct indicating viscometer for drilling fluids. American Petroleum Institute (API-54-007), New York.
24. Yıldız, N., Sarıkaya, Y. & Çalmlı, A. (1999). The characterization of Na₂CO₃ activated Kütahya bentonite. *Turkish Journal of Chemistry*, 23(3): 309-318.
25. Çinku, K., Boylu, F., Duman, F. & Çelik, M.S. (2010). The effect of the presence and amount of ions in the water on the product properties in the enrichment and activation of bentonites with soda. *Istanbul University Journal of Engineering Sciences*, 1(1), 9-18.
26. Karimi, L., Salem, A. (2011). Analysis of bentonite specific surface area by kinetic model during activation process in presence of sodium carbonate. *Microporous and mesoporous materials*, 141(3), 81-87.